A new class of scorpion toxin binding sites related to an A-type K^+ channel: pharmacological characterization and localization in rat brain

Hélène Vacher[a], Régine Romi-Lebrun[b], Christiane Mourre[c], Bruno Lebrun[b], Said Kourrich[c], Frédérique Masméjean[d], Terumi Nakajima[b], Christian Legros[e], Marcel Crest[f], Pierre E. Bougis[a], Marie-France Martin-Eauclaire[a,*]

[a] *UMR 6560 CNRS Université de la Mediterranée, Institut Jean Roche, Faculté de Médecine Nord, Boulevard Pierre Dramard, 13916 Marseille Cedex 20, France*
[b] *Suntory Institute for Bioorganic Research, Mishima-Gun, Shimanoto-Cho, Wakayamadai, Osaka, Japan*
[c] *UMR 6562 CNRS Université de Provence, Marseille, France*
[d] *LNCF CNRS, Marseille, France*
[e] *Institut für Neurale Signalverarbeitung, ZMNH Universität Hamburg, Hamburg, Germany*
[f] *ITIS, FRE 2362, Marseille, France*

Received 12 April 2001; accepted 30 May 2001

First published online 26 June 2001

Edited by Maurice Montal

Abstract A new scorpion toxin (3751.8 Da) was isolated from the *Buthus martensi* venom, sequenced and chemically synthesized (sBmTX3). The A-type current of striatum neurons in culture completely disappeared when 1 μM sBmTX3 was applied (K_d = 54 nM), whereas the sustained K^+ current was unaffected. ^{125}I-sBmTX3 specifically bound to rat brain synaptosomes (maximum binding = 14 fmol mg^{-1} of protein, K_d = 0.21 nM). A panel of toxins yet described as specific ligands for K^+ channels were unable to compete with ^{125}I-sBmTX3. A high density of ^{125}I-sBmTX3 binding sites was found in the striatum, hippocampus, superior colliculus, and cerebellum in the adult rat brain. © 2001 Published by Elsevier Science B.V. on behalf of the Federation of European Biochemical Societies.

Key words: A-type K^+ current; Scorpion toxin; Distribution in rat brain

1. Introduction

K^+ channels play crucial roles in many different cellular functions including cell excitability, neurotransmitter release, hormonal secretion, signal transduction, cell volume regulation, and neuronal integration [1]. Fast transient K^+ channels (transient A) are of particular interest because they regulate firing frequency, spike initiation and waveform of action potential [1]. Physiological studies show that A-type currents exhibit a wide range of biophysical and pharmacological properties, according to their cellular functions, as well as a molecular heterogeneity. Few specific blockers acting on A-type K^+ channels have been identified. They are heteropodatoxins (HpTX) and phrixotoxin (PaTX), from the spiders *Heteropoda venatoria* [2] and *Phrixotrichus auratus* [3], which block the Kv4.2/Kv4.3 channels; BDS I and II from the sea-anemone *Anemonia sulcata*, which block Kv3.4 [4]. In addition to being useful tools to characterize, classify and study the physiological roles of K^+ channels, analysis of these toxins provides a structural basis for the potential design of new pharmaceutical agents [4]. Thus, the characterization of new toxins, inhibitor of A-type currents, is expected to be informative about the role of sustaining channels in neural and cardiac tissue.

Recently, Aa1, a new blocker of fast K^+ currents from cerebellum granular cells was isolated from the venom of the scorpion *Androctonus australis* [5]. Here, we describe the chemistry, the pharmacology and the rat brain binding sites distribution of a *Buthus martensi* Karch scorpion toxin, BmTX3, which blocks an A-type current in neurons of striatum cells in culture.

2. Materials and methods

2.1. Venoms and toxins

The *B. martensi* venom was collected as described [6]. Kaliotoxin (KTX) and P05 from *Androctonus mauretanicus* were synthesized as described [7,8]. Charybdotoxin (ChTX), iberiotoxin (IbTX), and mast cell degranulating peptide (MCD peptide) were from Bachem; apamin was from Sigma; α-DTX was purified from *Dendroaspis angusticep* [9]. BDS-I and BDS-II from *A. sulcata* and recombinant noxiustoxin (rNTX) from *Centruroides noxius* were from Alomone Labs. HpTX1 from *H. venatoria* was from NPS Pharmaceuticals Inc.

2.2. Purification, amino acid composition and sequence determination of BmTX3

Purification conditions are described in figure legends. Amino acid compositions were determined as described [6]. 3 nmol of BmTX3 were *S*-carboxymethylated. Treatment with pyroglutamate aminopeptidase (Boehringer, Germany) unblocked the N-terminal glutamate residue before sequencing [10,11]. Toxicity in vivo was tested on 20 g male C57 Bl/6 mice by i.c.v. injection as described [12].

2.3. Chemical synthesis of BmTX3

Solid phase synthesis of BmTX3 was performed using the FastMoc program, as described [13]. The identity of synthetic and natural products was verified by amino acid analysis after acid hydrolysis, by a C18 RP HPLC co-injection experiment using a gradient from 5% to 45% of 0.1% trifluoroacetic acid in acetonitrile in 40 min with initial isocratic conditions for 3 min (the synthetic and natural products coeluted at 27.6 min) and using MALDI-TOF mass spectrometry.

2.4. Patch recording of striatal neurons in culture

For primary culture of striatal neurons, striata were dissected from

*Corresponding author. Fax: (33)-4-91 69 88 39.
E-mail: eauclaire.mf@jean-roche.univ-mrs.fr

0014-5793/01/$20.00
PII: S0014-5793(01)02620-5

18 day old Sprague–Dawley rat embryos and cultured according to Ref. [14]. Neurons were studied using whole cell patch clamp technique. The bath solution contained (in mM): 140 NaCl, 2 KCl, 0.8 $MgCl_2$, 1.8 $CaCl_2$, 0.4 Na_2HPO_4 and 10 HEPES, pH 7.3. sBmTX3 was applied under pressure with a broken pipette. Experiments were carried out at room temperature (20–24°C). Patch pipettes were filled with (in mM): 120 KCl, 10 NaCl, 2 $MgCl_2$, 0.56 $CaCl_2$, 1 EGTA and 10 HEPES, pH 7.4. Capacity transient compensation was routinely performed in the cell-attached mode before patch membrane rupture. In the whole cell voltage clamp configuration, capacitive transients and leakage currents were subtracted using a factored hyperpolarizing pulse, without additional transient or series resistance compensation.

2.5. Iodination of sBmTX3 and pharmacological tests

sBmTX3 (0.5 nmol) was iodinated using lactoperoxidase [15] and the free iodide eliminated as described [12]. Specific radioactivities of 2000 cpm/fmol were routinely obtained. Analysis of the mono or diiodo derivatives was followed by MALDI-TOF mass spectrometry.

Rat brain synaptosomal fraction P_2 (90 μg/assay in a total volume of 200 μl) was used for binding assays in binding buffer (20 mM Tris–HCl pH 7.4, 50 mM NaCl, 0.1% BSA). Non-specific binding was determined throughout in the presence of 0.1 μM unlabeled sBmTX3. Incubation was 1 h at 25°C. Reaction was stopped by dilution, adding 4 ml of wash buffer (20 mM Tris–HCl, pH 7.4, 150 mM NaCl, 1% BSA) and the solution was immediately filtered through a GF/C filter soaked in 0.1% polyethylenimine. Filters were washed twice and the filter-retained radioactivity was determined by γ-counting. Each point was made in triplicate. All the data were subjected to non-linear regression analysis using PRISM (GraphPad) and assuming the presence of a single class of binding sites.

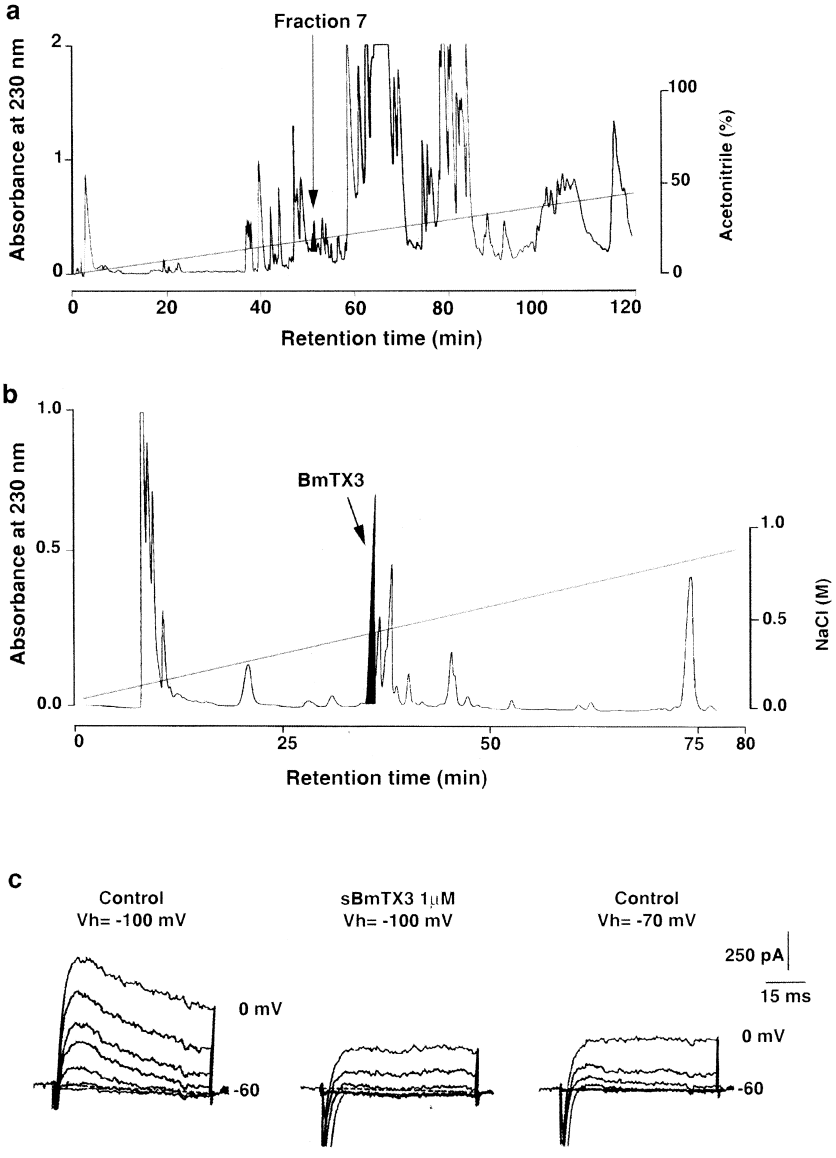

Fig. 1. Purification and electrophysiological testing of BmTX3. a: Reverse-phase C18 HPLC profile of the soluble venom (300 mg) from *B. martensi* scorpion. A linear gradient of 0.1% TFA–acetonitrile was applied on a semipreparative column Shiseido Capcell pak (25×1 cm, 120 Å, 5 μm) from 0 to 45% over 120 min at a flow rate of 3 ml min^{-1}. The component used for subsequent purification numbered 7 is in black. b: Purification of fraction 7 by cation exchange chromatography on a sulfopropyl column. 1/6 of fraction 7 was loaded on a cation exchange Tosoh, TSK-gel, sulfopropyl SP-5PW, 0.6×7 cm HPLC column in 10 mM sodium phosphate. A linear gradient from 0 to 800 mM NaCl, pH 6.8, was applied over 80 min at a flow rate of 0.5 ml min^{-1}. BmTX3 eluted by 490 mM NaCl. c: sBmTX3 blocks the A-current of the striatal neurons in culture. Total currents elicited from a V_h of −100 mV in control conditions and after application (17 min) of 1 μM of sBmTX3. Depolarization between −60 mV and 0 mV with steps of 10 mV. Currents recorded in the presence of sBmTX3 were compared to currents recorded from a V_h of −70 mV, a holding potential that inactivates the A-type current.

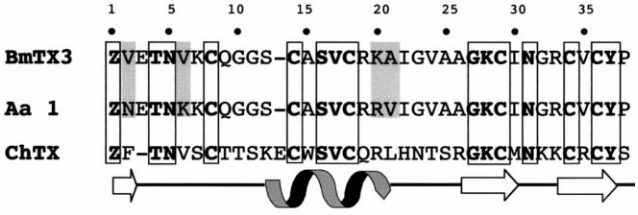

Fig. 2. Amino acid sequence of BmTX3. The sequence of BmTX3 is aligned with Aa 1 from *A. australis* [5] and ChTX from *Leiurus quinquestriatus hebraeus* [10] according to their half-cystine and gaps were introduced to enhance sequence similarities. Identities among the three sequences are boxed. Differences between BmTX3 and Aa 1 are in gray. Z indicates pyroglutamate. The arrows are β-strands and the helix is α-helix as observed for ChTX.

2.6. Autoradiographic procedures

Anaesthetized adult male Sprague–Dawley rats (150–200 g) were killed by decapitation, and their brains were removed and frozen. Sagittal cryostat sections (15 μm) were collected and stored at −60°C until use. The brain sections were incubated with 0.5 nM ^{125}I-sBmTX3 at 4°C in binding buffer. The non-specific binding component was measured by addition of 0.1 μM sBmTX3, 15 min before the addition of ^{125}I-sBmTX3. After a 60 min incubation, the sections were rinsed four times (with each wash lasting 30 s) in wash buffer and then rinsed once (3 s) in the same buffer containing 0.1% BSA. The dried slices were exposed to Kodak Biomax MR films that were processed after a 15 day exposure. Rat brain regions were identified according to the rat brain atlas [16].

3. Results

3.1. Purification, amino acid sequence determination, and chemical synthesis of BmTX3

The venom of the Chinese scorpion *B. martensi* was screened using HPLC, MALDI-TOF mass spectrometry and toxicological analysis. The fraction 7 (Fig. 1a) contained low molecular weight toxins, one of which (BmTX3) had a mass of 3751.8 Da (Fig. 1b). When injected in mice (8 μg i.c.v.), it caused epileptiform behavior. Its amino acid composition analysis gave the following ratios: 1.9 Asx (2); 3.0 Glx (3); 1.9 Ser (2); 5.3 Gly (5); 1.1 Thr (1); 4.1 Ala (4); 1.1 Pro (1); 2.1 Arg (2); 0.9 Tyr (1); 4.7 Val (5); 2.0 Ile (2); 3.0 Lys (3). It accounted for 0.06% of the dry mass of the venom. No PTH-amino acid was detected at the first step of the sequencing process of BmTX3, suggesting that it was blocked at its N-terminal extremity. The molecular mass of the native peptide was nearly 16 Da lower than that deduced from amino acid composition, including six putative cysteine residues (3768.3 Da). This difference was in accordance with the presence of a pyroglutamic acid residue at the N-terminus, as it is the case for ChTX. After treatment by pyroglutaminase, *S*-carboxymethylated BmTX3 was successfully sequenced. Thus, BmTX3 was composed of a single chain of 37 amino acid residues, most probably reticulated by three disulfide bridges since six carboxymethyl-cysteines were detected (Fig. 2). BmTX3 had 89% sequence homology with the recently described toxin Aa1

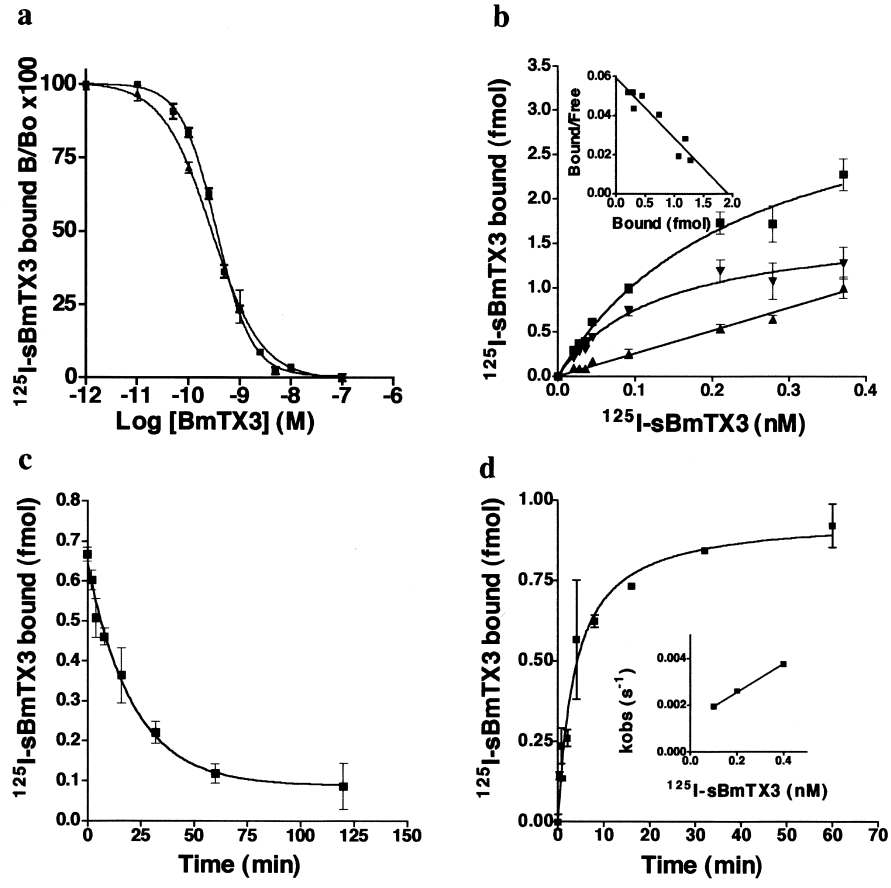

Fig. 3. Characterization of ^{125}I-sBmTX3 binding to rat brain P_2. a: Competitive binding of 400 pM ^{125}I-sBmTX3 with native BmTX3 (▲) or sBmTX3 (■). b: Equilibrium binding of ^{125}I-sBmTX3 (10–380 pM) to rat brain P_2: (■) total binding; non-specific binding (▲); specific binding (▼). Inset: Scatchard plot of the data. c: Dissociation was measured after incubation (1 h) of 400 pM ^{125}I-sBmTX3. d: Association of ^{125}I-sBmTX3 was measured as illustrated for 400 pM. k_{obs} values were determined for specific binding at 400, 200 and 100 pM (see inset).

from *A. australis* (α-KTX4.4) [5]. The N-terminal pyroglutamic acid and Tyr_{36} had already been found in the ChTX family (α-KTX1.1). The highly conserved region involved in channel recognition [7,17–19], i.e. the β-sheet 26–32, contained some important differences to other scorpion toxins blocking K^+ channels: Ile_{29} instead of Met and Arg_{32} instead of Lys.

BmTX3 was chemically synthesized on solid phase. Yields of assembly and cleavage were 85% and 60%, respectively. The yield of the oxidation step was 1.6% for synthetic toxin (sBmTX3). sBmTX3 showed the same amino acid composition as the natural toxin, the same molecular mass (3751.6 vs 3751.8 Da), and coeluted with the natural toxin as a single peak in HPLC. Therefore, synthetic sBmTX3 was used for further biological characterization.

3.2. Whole cell patch recording of striatal neurons in culture

The current blocked by sBmTX3 was characterized by performing whole cell patch recording using striatal neurons in primary cell culture. Fig. 1c shows the inward and the outward currents recorded in control conditions from two holding potentials (V_h) of −100 and −70 mV. From a V_h of −100 mV both the A-type current and the sustained K^+ current were activated. From a V_h of −70 mV the A-type current was inactivated and the sustained K^+ current slightly inactivated (almost unaffected). In the presence of sBmTX3 (1 μM) the A-type current completely disappeared whereas the sustained K^+ current remained unaffected. Dose–response experiments indicated a K_d of 54 nM (not shown).

3.3. Radioiodination of sBmTX3 and determination of the binding parameters

The single tyrosine residue of BmTX3 at the penultimate position allowed its radioiodination. MALDI-TOF mass spectrometry analysis of the product confirmed that only a monoiodo derivative was obtained (3876.3 Da).

^{125}I-sBmTX3 binding to rat brain P_2 was first evaluated in competition experiments using native BmTX3 and sBmTX3 which behaved identically (Fig. 3a). Both completely displaced ^{125}I-sBmTX3 from its binding site with IC_{50} values in the 0.22 nM range. Saturation experiments showed that ^{125}I-sBmTX3 associated in a concentration dependent manner (Fig. 3b). The specific binding (defined as the difference between the total ^{125}I-sBmTX3 binding and the binding in the presence of 100 nM unlabeled sBmTX3) was a saturable function of ^{125}I-sBmTX3 concentrations giving a K_d of 0.21 ± 0.05 nM and a B_{max} of 14 fmol mg^{-1} of protein ($n = 3$). The non-specific binding ranged from 35 to 45% of the total binding. Adding an excess (100 nM) of unlabeled sBmTX3 initiated dissociation of prebound ^{125}I-sBmTX3 from its site (Fig. 3c). The first order dissociation rate constant k_{off} was $6.0 \times 10^{-4} \pm 2.6 \times 10^{-4}$ s^{-1} ($n = 2$) giving a $t_{1/2}$ of 17 min. Incubation of rat brain P_2 with various concentrations of ^{125}I-sBmTX3 (0.4 nM, 0.2 nM and 0.1 nM) revealed a concentration and time dependent association of the toxin (Fig. 3d). The second order association rate constant k_{on} was $6.0 \times 10^6 \pm 0.2 \times 10^6$ M^{-1} s^{-1} ($n = 2$). The K_d value calculated from these kinetic constants was $k_{off}/k_{on} = 0.1$ nM, in good agreement with that determined under equilibrium binding conditions.

3.4. Competition experiments with other K^+ channel blockers

The Kv1. family blockers KTX, rNTX, ChTX (also blocker of the BKCa channel), MCD peptide and α-DTX (all up to 0.1 μM) did not compete with ^{125}I-sBmTX3. BDS-I and BDS-II which are blockers of Kv3.4 and HpTX1, a blocker of the Kv4.2/Kv4.3, were also unable to compete with ^{125}I-sBmTX3 (all up to 0.1 μM). Only apamin (a blocker of the SKCa channels) slightly displaced ^{125}I-sBmTX3 from its binding site but at doses > 1 μM. ^{125}I-sBmTX3 binding was inhibited by 15 mM TEA and 18 mM 4-AP. The inhibition of K^+ channels by TEA and 4-AP has been well documented [20,21].

3.5. Distribution of sBmTX3 binding sites in adult rat brain

The distribution of sBmTX3 binding sites in the rat brain was heterogeneous and the high grain levels predominated in very few structures (Fig. 4a,b). Non-specific binding was uniform in the different brain regions and no variation was detectable between the gray and the white matter (Fig. 4c). In the telencephalon, very high densities of sBmTX3 binding sites were present, in the caudate putamen and the accumbens nucleus whereas the neocortex, the globus pallidum, and the septum contained low to intermediate levels of binding sites. In the hippocampus, the sBmTX3 sites were not homoge-

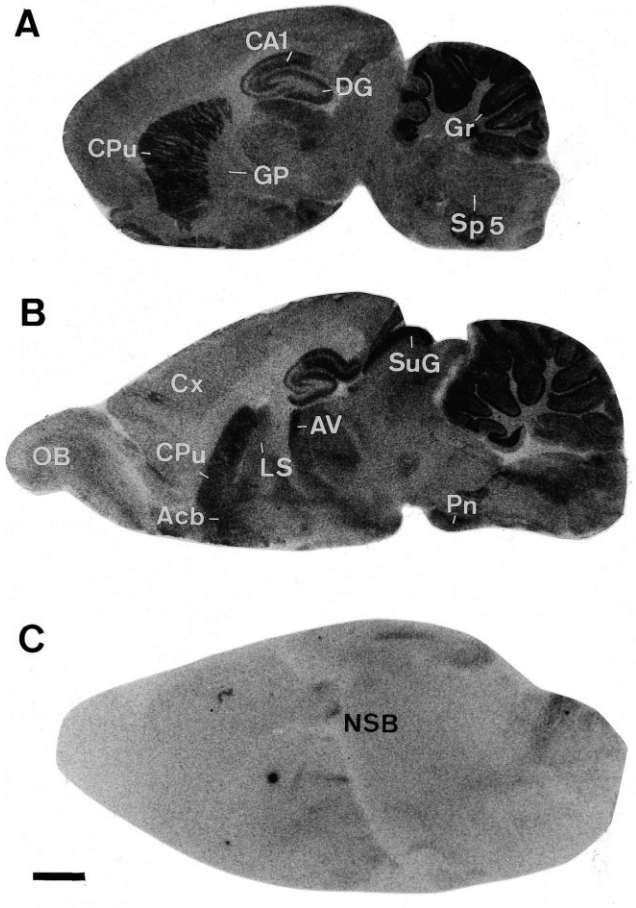

Fig. 4. Distribution of ^{125}I-BmTX3 binding sites in parasagittal sections of rat brain. In the autoradiograms, the dark areas indicate the high grain density, i.e. high binding site density. The non-specific binding (NSB) was homogeneous throughout the brain. Bar = 2 mm. Abbreviations: Acb, accumbens nucleus; AV, anteroventral thalamic nucleus; CA1, field 1 of Ammon's horn; CPu, caudate putamen; Cx, neocortex; DG, dentate gyrus; GP, globus pallidus; Gr, granular layer of the cerebellum; LS, lateral septum; OB, olfactory bulb; Pn, pons; Sp5, spinal trigeminal nucleus; SuG, superior colliculus.

neously distributed. The strati oriens and radiatum of the CA1 and CA3 field were more heavily labeled with high densities than the stratum lacunosum moleculare. The molecular layer of the dentate gyrus also presented high densities of sBmTX3 sites. In the subiculum, the density of sites was low. There were few sites in the rhinenchephalon, however the anterior olfactory nucleus showed an intermediate labeling. In the diencephalon, an intermediate level of sBmTX3 binding sites was observed in the thalamic nuclei particularly in the anterior nucleus whereas the specific binding, in the other regions, was very low in particular in the hypothalamus. In the mesencephalon, the density of sBmTX3 sites was homogeneous and low except in the superior colliculus where labeling was dense. The metencephalon was weakly labeled. In the medulla, only the pontine nuclei presented an intermediate level of sites whereas the other structures contained low levels. The cerebellum showed a heterogeneous distribution of the sBmTX3 binding sites with a high density in the granular layer, an intermediate density in the molecular layer, and no labeling in the fiber tracts. At histological resolution, labeling in the Purkinje cell layer could not be excluded. In the white matter, there was no detectable difference between the total and the non-specific binding.

4. Discussion

4.1. BmTX3 and Aa1 define a new group of transient K^+ current blocker

The chemical and electrophysiological data concerning sBmTX3 are in agreement with the results obtained with Aa1, which blocks transient K^+ currents in cerebellum granular cells with a K_d around 150 nM [5]. At the amino acid sequence level, BmTX3, like Aa 1, contains the conserved structural signature of scorpion toxins, i.e. an α-helix linked to an antiparallel β-sheet [22]. Interestingly, among the five residues in the β-sheet generally involved in the binding of KTX, AgTX2 and ChTX to the *Shaker* [17,18], Kv1.3 [7,19] or BK channels [23], only three (Lys_{27}, Asn_{30} and Tyr_{36}) are conserved in BmTX3. Nevertheless, BmTX3 retains the ability to recognize some K^+ channels.

Our electrophysiological experiments demonstrate that sBmTX3 blocks a transient (A-type) K^+ current expressed in culture of striatal neurons. The striatum contains the caudate putamen, a region with a high density of ^{125}I-sBmTX3 binding sites. These cultures contain numerous gabaergic neurons and some cholinergic neurons [14]. To our knowledge, no information is available concerning the nature of the subunits constituting the transient K^+ current in striatal gabaergic neurons. However, striatal cholinergic interneurons contains mRNAs for Kv1.4, Kv4.1 and Kv4.2 subunits [24].

4.2. BmTX3 defines a new pharmacological binding site in rat brain

^{125}I-sBmTX3 is able to bind to specific sites in rat brain with a high affinity. The same affinities are obtained comparing ^{125}I-sBmTX3 binding and its competitive displacement by BmTX3. This suggests that the iodination of BmTX3 does not alter its activity. This result is significant as it was observed for ChTX [25] and HgTX [26] that a bulky hydrophobic iodine at Tyr_{37} reduces the affinity of the toxin. The density of binding sites is lower (14 fmol mg^{-1} of protein) than those of ^{125}I-α-DTX (500–1100 fmol mg^{-1} of protein) and ^{125}I-MCD peptide (160 fmol mg^{-1} of protein) in identical rat brain synaptosomal fractions [27]. It is difficult to compare the number of binding sites with those of other toxins (^{125}I-ChTX or ^{125}I-HgTX), due to differences in the characteristics of the rat brain fractions used. However, this density of BmTX3 binding sites is in the same range as those found for KTX (24 fmol mg^{-1} of protein) and for apamin (12.5 fmol mg^{-1} of protein) [28]. The sites detected were found to be highly specific for ^{125}I-sBmTX3. The binding was not inhibited by any of the K^+ channel peptidic blockers described.

4.3. BmTX3 defines a new localization pattern in rat brain

Interestingly, the distribution of ^{125}I-sBmTX3 binding sites in adult rat brain is highly heterogeneous, suggesting a neuronal labeling. However, the presence of ^{125}I-sBmTX3 binding sites in astrocytes cannot be excluded. This distribution with high site densities in caudate putamen, is very different from those of other peptidyl K^+ channels toxins. Indeed, except in hippocampus and cerebellum, DTX I, α-DTX and MCD peptide binding sites are evenly distributed in the gray matter [27,29,30]. ^{125}I-KTX binding sites present a high density in the neocortex, hypothalamus, stria terminalis, and parabrachial nucleus and a low level in caudate putamen [31]. For MgTX, most of the brain regions contain a homogeneous level of binding sites, with the exception of major fiber tracts where the highest density is detected [32]. For apamin, high binding is detected in hippocampus, but also in thalamus and in septum where the levels of ^{125}I-sBmTX3 binding sites are low [33]. For ChTX, binding is moderate in caudate putamen and in hippocampus but very high in hypothalamus and mesencephalum [34].

4.4. Concluding remarks

Autoradiographic experiments show that few structures in the rat brain contain high densities of ^{125}I-sBmTX3 binding sites. The fact that the distribution of these sites is very different from those of others toxins acting on K^+ channels is consistent with BmTX3 recognizing a channel type insensitive to other known toxins. As a high density of ^{125}I-sBmTX3 binding sites is found in the granular layer of the cerebellum, we suppose that sBmTX3 and Aa1 recognize the same target in rat brain. Accordingly, BmTX3 and Aa1 may constitute the first members of a new family of short chain scorpion toxins active on transient K^+ channels [35].

Acknowledgements: We thank Dr. P. Marchot for providing purified α-DTX and G. Jacquet for helpful in patch-clamp experiments. This study was supported by a grant from the DGA to H.V.

References

[1] Coetzee, W.A. et al. (1999) Ann. N. Y. Acad. Sci. 868, 233–285.
[2] Sanguinetti, M.C., Johnson, J.H., Hammerland, L.G., Kelbaugh, P.R., Volkmann, R.A., Saccomano, N.A. and Mueller, A.L. (1997) Mol. Pharmacol. 51, 491–498.
[3] Diochot, S., Drici, M.D., Moinier, D., Fink, M. and Lazdunski, M. (1999) Br. J. Pharmacol. 126, 251–263.
[4] Diochot, S., Schweitz, H., Beress, L. and Lazdunski, M. (1998) J. Biol. Chem. 273, 6744–6749.
[5] Pisciotta, M., Coronas, F.I., Bloch, C., Prestipino, G. and Possani, L.D. (2000) Biochim. Biophys. Acta 1468, 203–212.
[6] Romi-Lebrun, R., Martin-Eauclaire, M.F., Escoubas, P., Wu, F.Q., Lebrun, B., Hisada, M. and Nakajima, T. (1997) Eur. J. Biochem. 245, 457–464.
[7] Romi, R. et al. (1993) J. Biol. Chem. 268, 26302–26309.

[8] Sabatier, J.M., Zerrouk, H., Darbon, H., Mabrouk, K., Benslimane, A., Rochat, H., Martin-Eauclaire, M.F. and Van Rietschoten, J. (1993) Biochemistry 32, 2763–2770.
[9] Tricaud, N., Marchot, P. and Martin-Eauclaire, M.F. (2000) Toxicon 38, 1749–1758.
[10] Gimenez-Gallego, G., Navia, M.A., Reuben, J.P., Katz, G.M., Kaczorowski, G.J. and Garcia, M.L. (1988) Proc. Natl. Acad. Sci. USA 85, 3329–3333.
[11] Galvez, A., Gimenez-Gallego, G., Reuben, J.P., Roy-Contancin, L., Feigenbaum, P., Kaczorowski, G.J. and Garcia, M.L. (1990) J. Biol. Chem. 265, 11083–11090.
[12] Laraba-Djebari, F. et al. (1994) J. Biol. Chem. 269, 32835–32843.
[13] Romi-Lebrun, R. et al. (1997) Biochemistry 36, 13473–13482.
[14] Kowalski, C., Crest, M., Vuillet, J., Pin, T., Gola, M. and Nieoullon, A. (1995) Neuroscience 64, 979–993.
[15] Rochat, H., tessier, M., Miranda, F. and Lissitzky, S. (1976) in: Animal, Plant, and Microbial Toxins, Vol. 1, pp. 81–88, Plenum, New York.
[16] Paxinos, G. and Watson, C. (1986), Academic Press, New York.
[17] Park, C.S. and Miller, C. (1992) Biochemistry 31, 7749–77455.
[18] MacKinnon, R., Cohen, S.L., Kuo, A., Lee, A. and Chait, B.T. (1998) Science 280, 106–109.
[19] Aiyar, J. et al. (1995) Neuron 15, 1169–1181.
[20] MacKinnon, R. and Yellen, G. (1990) Science 250, 276–279.
[21] Heginbotham, L., Abramson, T. and MacKinnon, R. (1992) Science 258, 1152–1155.
[22] Bontems, F., Roumestand, C., Gilquin, B., Menez, A. and Toma, F. (1991) Science 254, 1521–1523.
[23] Goldstein, S.A., Pheasant, D.J. and Miller, C. (1994) Neuron 12, 1377–1388.
[24] Song, W.J., Tkatch, T., Baranauskas, G., Ichinohe, N., Kitai, S.T. and Surmeier, D.J. (1998) J. Neurosci. 18, 3124–3137.
[25] Tenenholz, T.C., Klenk, K.C., Matteson, D.R., Blaustein, M.P. and Weber, D.J. (2000) Rev. Physiol. Biochem. Pharmacol. 140, 135–185.
[26] Koschak, A., Bugianesi, R.M., Mitterdorfer, J., Kaczorowski, G.J., Garcia, M.L. and Knaus, H.G. (1998) J. Biol. Chem. 273, 2639–2644.
[27] Bidard, J.N., Mourre, C., Gandolfo, G., Schweitz, H., Widmann, C., Gottesmann, C. and Lazdunski, M. (1989) Brain Res. 495, 45–57.
[28] Hugues, M., Duval, D., Kitabgi, P., Lazdunski, M. and Vincent, J.P. (1982) J. Biol. Chem. 257, 2762–2769.
[29] Mourre, C., Bidard, J.N. and Lazdunski, M. (1988) Brain Res. 446, 106–112.
[30] Awan, K.A. and Dolly, J.O. (1991) Neuroscience 40, 29–39.
[31] Mourre, C., Chernova, M.N., Martin-Eauclaire, M.F., Bessone, R., Jacquet, G., Gola, M., Alper, S.L. and Crest, M. (1999) J. Pharmacol. Exp. Ther. 291, 943–952.
[32] Saria, A. et al. (1998) Eur. J. Pharmacol. 343, 193–200.
[33] Mourre, C., Hugues, M. and Lazdunski, M. (1986) Brain Res. 382, 239–249.
[34] Gehlert, D.R. and Gackenheimer, S.L. (1993) Neuroscience 52, 191–205.
[35] Tytgat, J., Chandy, K.G., Garcia, M.L., Gutman, G.A., Martin-Eauclaire, M.F., van der Walt, J.J. and Possani, L.D. (1999) Trends Pharmacol. Sci. 20, 444–447.